The wimple: A rippled deformation of a wetting film during its drainage

Vladimir S. Ajaev
Department of Mathematics, Southern Methodist University, Dallas, Texas 75275

Roumen Tsekov and Olga I. Vinogradova
A. N. Frumkin Institute of Physical Chemistry and Electrochemistry, Russian Academy of Sciences, 31 Leninsky Prospect, 119991 Moscow, Russia

(Received 27 February 2007; accepted 24 April 2007; published online 19 June 2007)

It has long been accepted that hydrodynamic pressure in a draining fluid film can cause inversion of curvature of a fluid-fluid interface, creating the so-called dimple. However, it was recently discovered that a different shape, dubbed a wimple, can be formed if a bubble/drop is initially in the field of repulsive surface forces, so that a wetting film is formed. The film profile then includes a central region in which the film remains thin, surrounded by a ring of greater film thickness and bounded at the outer edge by a barrier rim. This shape later evolves to a conventional dimple, which then drains in the usual way. Here we carry out numerical simulations of the draining film evolution that allow us to uncover the physical mechanism responsible for wimple formation. Simple analytical estimates are then obtained for characteristic times of different stages of drainage, and are shown to be in good agreement with experimental data. We demonstrate that wimpling is a general phenomenon that can be encountered in many different systems. © *2007 American Institute of Physics*. [DOI: 10.1063/1.2741151]

Studies of hydrodynamic interactions involving drops and bubbles are vitally important for describing the behavior of emulsions and foams, flotation processes, coalescence and fusion phenomena, as well as for modelling the behavior of biological systems, such as membranes and perhaps even living cells. When a bubble or a liquid drop surrounded by another viscous liquid is pressed against a solid wall, a thin draining film is formed. Despite some, mostly technical, complications in the quantitative description of complex deformable interfaces, the qualitative picture and the underlying physics of a thin film drainage appeared to be fully understood several decades ago. It has been believed that when the approach speed is sufficiently high and the separation is small, the hydrodynamic pressure in the film can be large enough to invert the curvature of a fluid drop or a bubble, forming the so-called dimple.[1–3] The dimple is bounded by a barrier rim, which is the circle of minimum separation between the two surfaces. The rate at which fluid can flow through the thin gap at the barrier rim restricts the film drainage, and this can become the rate-limiting process in determining many phenomena. The dimpling has been confirmed in numerous macroscopic experiments and predicted theoretically.[4–7] Qualitatively similar film profiles have also been observed at the submicroscopic scale, where a disjoining pressure and relevant surface forces become important.[8–10] However, an entirely new observation has been made in a recent experiment,[11] revealing that at the nanoscale the commonly accepted notions about the shape evolution of a draining film are incomplete. The new result is that if the substrate starts to move toward drop/bubble from an equilibrium configuration, a more complex rippled shape, a wimple, can be observed at the initial stage of approach (Fig. 1). In a wimple, the wetting film thickness has a depression near the axis of symmetry ($r=0$) surrounded by a ring of greater film thickness and bounded at the outer edge by a barrier rim (see also Fig. 2). This shape later evolves to a conventional dimple, which then drains in the usual way. Rippled dissipative structures, e.g., surface waves, are often observed in large scale systems. They have also been detected at the nanoscale, being inevitably attributed to various types of instabilities.[13–15] It is, however, striking to discover similar phenomena in essentially stable nanofilms, where the surface tension and positive disjoining pressure are expected to suppress any wave-like deformations.[11] The purpose of the present Letter is to outline a physical mechanism responsible for a rippled deformation of a draining wetting film.

Consider an axisymmetric bubble pressed against a horizontal rigid surface, which is a typical experimental configuration,[10,11,16,17] illustrated in Fig. 2. Liquid has viscosity μ and surface tension at the liquid-gas interface is σ. The bubble is held at the end of a fixed vertical capillary, while the solid substrate can be moved in the vertical direction at a controlled velocity. When the bubble is far from the solid wall, its radius of curvature is constant and equal to R_0, assuming that gravity can be neglected, i.e., the Bond number is small. When the bubble is close to the wall its shape is distorted locally by surface and hydrodynamic forces, resulting in the formation of a liquid film between the gas and the solid. When the substrate moves toward the capillary, the film region expands at a rate characterized by the velocity of its outer edge, U, used as the horizontal velocity scale in our model. The interplay between viscous flow and surface tension in the liquid film is described by the so-called Landau-Levich-Bretherton scaling,[12] which in the present context implies using $C^{1/3}R_0$ and $C^{2/3}R_0$ as the local length scales in the radial and vertical directions, respectively; $C=\mu U/\sigma$ is the capillary number. The scaled cylindrical coordinates, r and z, are shown in Fig. 2. The leading-order stress boundary conditions imply zero shear stress at the interface and the normal pressure jump in the form

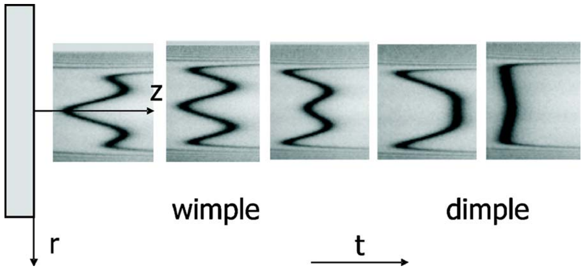

FIG. 1. Experimental recording of multiple beam interference fringes reflecting the wimple shape of the film and its evolution to a dimple, courtesy of L Y. Clasohm. Coordinate axes shown in the first snapshot are along the axis of symmetry (z) and in the radial direction along the solid wall (r).

$$p_g - p = h_{rr} + r^{-1}h_r + \Pi(h), \tag{1}$$

where p_g and p are the pressures inside the bubble and in the liquid film, respectively, $\Pi(h)$ is the scaled disjoining pressure. While several different components of disjoining pressure may be present in the experiment,[16,17] the mechanism discussed in the present study turns out to not be very sensitive to the particular choice of the expression for $\Pi(h)$. Below we use the standard London-van der Waals model, i.e., assume $\Pi(h)=\alpha h^{-3}$, where $\alpha=-A/\sigma C^2R_0^2$, A is the Hamaker constant.

The standard lubrication-type analysis[18] results in the equation for the rescaled liquid film thickness $h=h(r,t)$ in the form

$$h_t + (3r)^{-1}[rh^3(h_{rr} + r^{-1}h_r + \alpha h^{-3})_r]_r = 0, \tag{2}$$

where time is scaled by $C^{1/3}R_0/U$.

The boundary conditions for this equation at $r=0$ are the conditions of axial symmetry expressed by $h_r(0,t)=0$, $h_{rrr}(0,t)=0$. The right end of the domain, $r=L$, is defined by the condition that $h(L,t)=h_0$, where L can be changing with time when the computational domain is expanding to simulate the expansion of the flattened region of the bubble surface. The value of h_0 is chosen large enough so that $r=L$ is in the region where the interface is dominated by capillary forces and disjoining pressure is negligible. Finally, the condition for matching of the film curvature with that of the meniscus is written in the form

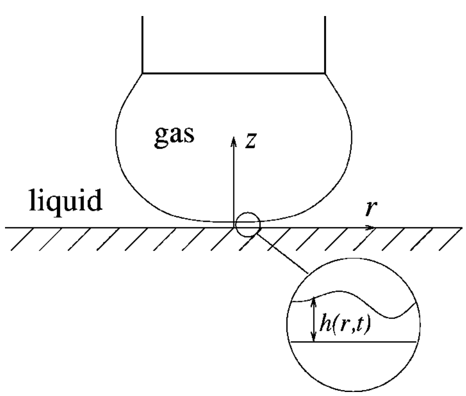

FIG. 2. Sketch of a bubble held in a fixed capillary and pressed against a solid surface. Wimple shape is illustrated in the enlarged view of the wetting film region.

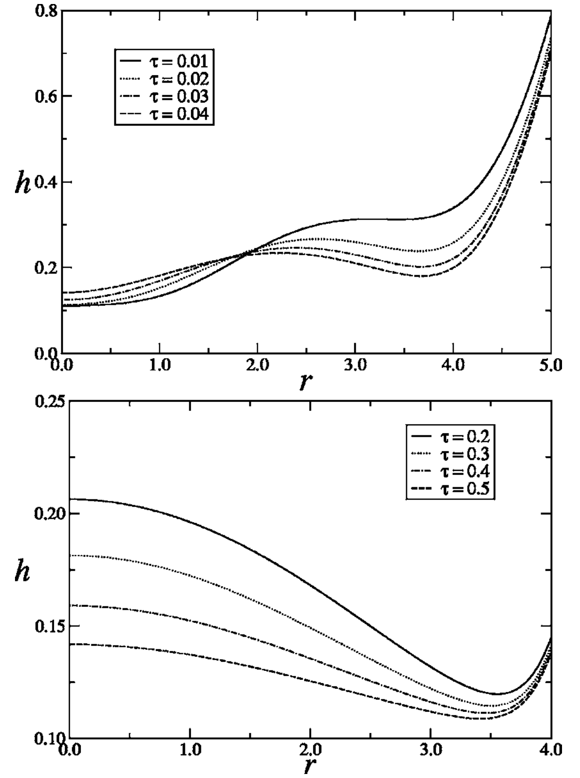

FIG. 3. Numerical results for $\alpha=10^{-3}$ illustrating liquid-gas interface evolution: (top) formation of the wimple; (bottom) drainage of the dimple at the later stages of evolution.

$$h_{rr}(L,t) + L^{-1}h_r(L,t) = 1. \tag{3}$$

Note that $L=L(t)$. Equation (2) with the specified boundary conditions was solved numerically using a finite difference approach with time stepping based on Gear's backward differentiation formulas.

There exists a possibility of a steady configuration, when the disjoining pressure in the wetting film balances the capillary pressure jump across the meniscus interface. This configuration is taken as the initial condition, and the right end point of the computational domain is moved a distance ΔL at a constant speed, i.e., $L(t)=L(0)+t$, which in the framework of the small capillary number approximation simulates the step-like change in the distance between the bubble and the wall. (We note that there is an issue with applicability of such models since flow accelerations have to remain bounded. We therefore also ran simulations using a large but finite rate of change of velocity and found that the behavior of the system over the time scales of interest does not change significantly.) Figure 3 (top) shows typical simulation results [for $\alpha=0.001$, $L(0)=3$, $\Delta L=3$] at the initial stages of the process. Snapshots of the interface are recorded at several different values of rescaled time $\tau=\alpha t$ specified in the legend. The extent of the wetting film does not change very significantly, but the meniscus moves a significant distance to the right, resulting in the formation of a trailing film. A depression is then formed in this film, resulting in a shape with a minimum at the axis of symmetry and another minimum at a finite r, i.e., a wimple.

At later stages of evolution the wimple transforms into the standard dimple shape[5,6,19] and the latter slowly relaxes

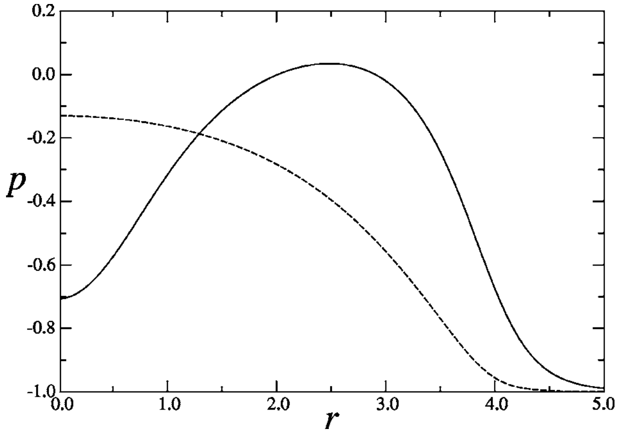

FIG. 4. Pressure distributions for the wimple (τ=0.03, solid line) and the dimple (τ=0.3, dashed line).

to the flat film, as illustrated in Fig. 3 (bottom). This turns out to be a much slower process than the initial evolution, and it is completed long after the substrate stopped moving.

The flow in the liquid film is driven by a combination of gradients of the capillary and disjoining pressures, so a useful insight into the nature of the flow can be obtained by investigating the evolution of the total scaled pressure, computed from Eq. (1) where for simplicity we set the (constant) pressure in the gas, p_g, to zero. Typical plots of the total pressure for dimple and wimple are shown in Fig. 4. The maximum of pressure for the dimple is at the axis of symmetry, while the highest pressure for the wimple shape is attained at a circular ring.

Based on the above simulations, we propose the following general mechanism for wimple formation. In equilibrium, the disjoining pressure in the wetting film, point A in Fig. 5 (top), balances the capillary pressure jump across the meniscus (B), so that $p_A = p_B$. When the meniscus starts moving, the trailing film is formed by the Landau-Levich-type mechanism; the typical thickness of this film scales as $C^{2/3}$. This thickness is larger than the wetting film thickness, so the disjoining pressure in this film, region B in Fig. 5 (bottom), is relatively small. But the capillary pressure jump is also small, since the trailing film is almost flat when it is newly formed. Thus, there is a region of increased pressure, $p_B > p_A$ and $p_B > p_C$, and as a result the liquid is pushed out of this region in both directions, i.e., toward the capillary meniscus region and toward the wetting film, resulting in formation of the wimple.

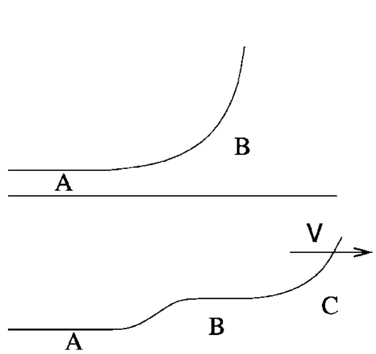

FIG. 5. A sketch of the physical mechanism of wimple formation.

An important aspect of the wimpling is that it can only occur if some of the fluid in the film first flows towards the central axis, before later draining in the opposite direction.[11] Indeed, the flow direction is associated with the pressure in the film, which in turn can be related to the shape of the interface. Hence, when a wimple is present the film pressure at the center and near the shoulder (or barrier rim) is low, while it is high in the intermediate annular region where curvature is concave. Therefore, when the drop/bubble is pushed fast towards the wall, the response of the film is first to flow inward toward the central region, before later reversing the flow and draining out again. We propose that a reversal of the radial flow direction during thin film drainage is the norm rather than the exception and note that this effect may have potential applications for mixing at the nanoscale.

To make a better connection to experimental work it is useful to interpret our numerical results in dimensional terms. At the characteristic speed of $U = 100\ \mu\mathrm{m/s}$, the value of $C^{1/3}$ is typically on the order of 10^{-2}. Thus, for the bubble of radius 1 mm, the orders of magnitude for dimensional radial and vertical scales in the draining film region are 10 μm and 100 nm, respectively. Direct comparison of our work with experiment is difficult since the experimental recording of wimple shape[11] was obtained for a droplet of mercury instead of an air bubble so the flow inside the droplet may have an effect on the process and our simple disjoining pressure model may not describe the experimental situation accurately enough. However, the main features of the proposed mechanism, such as formation of stable wetting film and a thicker and nearly flat trailing film, are the same in this case. Furthermore, we expect the flow in the film to be the limiting mechanism for the dynamics of the system. Our estimates of the dimensional time are consistent with the time scales of the shape evolution in experiments. Indeed, if we use the surface tension at the water-mercury interface and viscosity of water, but ignore the effects of flow in the mercury, the characteristic time $C^{1/3}R_0/U$ is near 0.06 s. Then the dimensional time of wimple formation is estimated to be 0.5 s, transition to dimple occurs at 5 s, and the dimple disappears after 50 s. This can be compared with the experimental values of 0.44 s, 3.8 s, and 34 s in Fig. 2 in Ref. 11. While this comparison is qualitative, it provides justification for the physical mechanism proposed in the present work.

In addition to numerical predictions it is also useful to obtain simple analytical estimates of the typical time scales of a wimple formation and a dimple drainage. These can be done by linearizing Eq. (2),

$$h_t + (3r)^{-1}\bar{h}^3[r(h_{rr} + r^{-1}h_r - 3\alpha\bar{h}^{-4}h)_r]_r = 0, \tag{4}$$

where $\bar{h}$ denotes the average film thickness. The solution of Eq. (4) on $[0,L]$ can be written as a linear superposition in the form

$$h = \bar{h} + \sum_n A_n e^{-\gamma_n t} J_0(q_n r). \tag{5}$$

Since the average value over r of the sum over n on the right-hand side has to vanish, the dimensionless wavenumbers q_n obey the relationship $J_1(q_n L) = 0$, based on the well-known relation between Bessel functions of the zeroth and the first orders. Thus, $q_n=\lambda_n/L$, where λ_n is the nth root of the Bessel function of the first kind, J_1. The dimensionless decay rate γ_n satisfies the following dispersion relation:

$$\gamma_n=(\bar{h}^3q_n^2/3)(q_n^2+3\alpha\bar{h}^{-4}). \tag{6}$$

Note that with the increase in n, q_n grows linearly, while γ_n grows biquadratically. In general, at a given time many wavenumbers are present. However, the short wavelength (large n) perturbations decay rapidly with time, so only perturbations that correspond to the smallest values of n remain. Hence, they determine primarily the shape of the film for large time t. Equation (6) can be used to gain insights into the time evolution of interface shapes. At very large times the film reaches flat equilibrium shape, which corresponds to perturbations of all wavelengths decaying to zero. At the late stages of the shape evolution (relatively large t), the film is not yet at equilibrium, but already close to it. Thus, the Fourier components with large γ_n are also decaying, but the film is not flat yet due to the component $n=1$. Then the interface shape is essentially dimpled with a characteristic wavenumber $q_1=\lambda_1/L$. Since $\lambda_1\approx 3.83$, the dimple has a maximum in the film center and a minimum at the rim. The rescaled decay time $\gamma_1^{-1}\alpha$ is close to 0.3, giving an estimate of the drainage time consistent with the simulation data. If we now consider the shape evolution before the dimple formation, we can expect that $q_2=\lambda_2/L$ will also play an important role. The value $\lambda_2\approx 7.02$ corresponds to a wimple with a maximum surrounded by two minima at the center and the rim. The corresponding evolution time $\gamma_2^{-1}\alpha\sim 0.05$, which is also in good agreement with the simulations.

Based on the analysis of interfacial stress conditions, it has been predicted that rippled deformations can appear as a result of interplay between surface tension and disjoining pressure.[20] In this earlier paper the wimple-dimple transition was discussed based on the assumption that the interface shape is dominated by a single Fourier component of the superposition given by Eq. (5); the wavenumber of that component was denoted by $\sqrt{b}$ in Ref. 20. The wimple shape then corresponds to larger values of b, while the dimple is expected at smaller b, with the transition between the two taking place when b is near the square of a root of the Bessel function J_1. Comparing this approach with the present study shows that b can be expressed in our notation as $b=q_1^2$ and therefore the condition $q_1=\lambda_1/L$ that we used in our estimate of wimple-dimple transition time is the same as the condition for b obtained in Ref. 20.

The rippled deformations behind moving menisci are crucial for understanding the dynamics of receding contact lines. The well-known dependence of dynamic contact angle correction on $C^{1/3}$ suggests that the Landau-Levich-Bretherton-type mechanism may play a role in contact line dynamics, but the connection between the two has not been fully understood. The present theory shows that the interplay between the ultrathin wetting film and the thicker trailing film behind the contact line is an essential feature of the dynamics of receding contact lines.

According to the above mechanism, we claim that the wimple is a generic phenomenon encountered en route to the dimple and applicable to the bubble/drop interactions, as well as in experiments on receding contact lines. We have shown that the inward-then-outward flow in the film is not a consequence of fluid inertia in the drop/bubble or of coupled flow of the film to internal circulation within the drop/bubble. It is not caused by high surface tension, a special type of disjoining pressure isotherm, or high density of the drop.

This work was partly supported by a DFG priority program "Micro and nanofluidics" (Contract No. Vi 243/1-2) and by the National Science Foundation under Grant No. CTS-0244676. We thank L. Y. Clasohm for providing experimental pictures used in Fig. 1.

[1] B. V. Derjaguin and M. M. Kussakov, "Anomalous properties of thin polymolecular films," Acta Physicochim. URSS **10**, 25 (1939).
[2] D. Platikanov, "Experimental investigation on the dimpling of thin liquid films," J. Phys. Chem. **68**, 3619 (1964).
[3] S. Hartland, "The effect of circulation patterns on the drainage of the film between a liquid drop and a deformable liquid-liquid interface," Chem. Eng. Sci. **65**, 82 (1969).
[4] S. P. Frankel and K. J. Mysels, "On the dimpling during the approach of two interfaces," J. Phys. Chem. **66**, 190 (1962).
[5] C.-Y. Lin and J. C. Slattery, "Thinning of a liquid film as a small drop or bubble approaches a solid plane," AIChE J. **28**, 147 (1982).
[6] S. G. Yiantsios and R. H. Davis, "On the buoyancy-driven motion of a drop towards a rigid surface or a deformable surface," J. Fluid Mech. **217**, 547 (1990).
[7] R. Tsekov and E. Evstatieva, "A fractal classification of the drainage dynamics in thin liquid films," Prog. Colloid Polym. Sci. **126**, 93 (2004).
[8] B. V. Derjaguin, N. V. Churaev, and V. M. Muller, *Surface Forces* (Plenum, New York, 1987).
[9] J. N. Israelachvili, *Intermolecular and Surface Forces* (Academic, London, 1992).
[10] J. N. Connor and R. G. Horn, "The influence of surface forces on thin film drainage between a fluid drop and a flat solid," Faraday Discuss. **123**, 193 (2003).
[11] L. Y. Clasohm, J. N. Connor, O. I. Vinogradova, and R. G. Horn, "The 'Wimple' rippled deformation of a fluid drop caused by hydrodynamic and surface forces during thin film drainage," Langmuir **21**, 8243 (2005).
[12] V. S. Ajaev and G. M. Homsy, "Modeling shapes and dynamics of confined bubbles," Annu. Rev. Fluid Mech. **38**, 277 (2006).
[13] A. M. Cazabat, F. Heslot, S. M. Troian, and P. Carles, "Fingering instability of thin spreading films driven by temperature gradients," Nature (London) **346**, 824 (1990).
[14] S. M. Troian, E. Herbolzheimer, and S. A. Safran, "Model for the fingering instability in spreading surfactant drops," Phys. Rev. Lett. **65**, 333 (1990).
[15] S. Herminghaus, R. Seemann, and K. Jacobs, "Generic morphologies of viscoelastic dewetting fronts," Phys. Rev. Lett. **89**, 056101 (2002).
[16] R. A. Pushkarova and R. G. Horn, "Surface forces measured between an air bubble and a solid surface in water," Colloids Surf., A **261**, 147 (2005).
[17] J. N. Connor and R. G. Horn, "Measurement of aqueous film thickness between charged mercury and mica surfaces: A direct experimental probe of the Poisson-Boltzmann distribution," Langmuir **17**, 7194 (2001).
[18] A. Oron, S. H. Davis, and S. G. Bankoff, "Long-scale evolution of thin liquid films," Rev. Mod. Phys. **69**, 931 (1997).
[19] R. Tsekov, P. Letocart, E. Evstatieva, and H. J. Schulze, "Effect of ionic surfactants on the dimple relaxation in wetting films," Langmuir **18**, 5799 (2002).
[20] R. Tsekov and O. I. Vinogradova, "A qualitative theory of wimples in wetting films," Langmuir **21**, 12090 (2005).